

Combinational Delivery of Hydrophobic and Hydrophilic Anticancer Drugs in Single Nanoemulsions To Treat MDR in Cancer

Yan Ma,^{‡,||} Dan Liu,^{§,||} Dun Wang,[§] Yongjun Wang,[§] Qiang Fu,[§] John K. Fallon,[†] Xinggang Yang,[§] Zhonggui He,[§] and Feng Liu^{*,†}

[†]Division of Molecular Pharmaceutics and Center for Nanotechnology in Drug Delivery, Eshelman School of Pharmacy, University of North Carolina at Chapel Hill, Chapel Hill, North Carolina 27599, United States

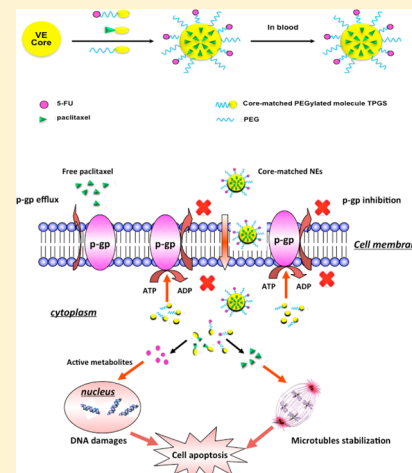
[‡]School of Chinese Materia Medica, Guangzhou University of Chinese Medicine, Guangzhou 510006, China

[§]Shenyang Pharmaceutical University, Shenyang 110016, China

Supporting Information

ABSTRACT: In this study, we developed the core-matched nanoemulsions (NEs) functionalized by vitamin E (VE) and tocopherol poly(ethylene glycol)succinate (TPGS) to codeliver hydrophobic and hydrophilic drugs, paclitaxel (PTX) and 5-fluorouracil (5-FU), in order to achieve synergistic effects and overcome PTX resistance in a multi-drug-resistant (MDR) human epidermal carcinoma cell line KB-8-5. Antitumor effect of the combination therapy based on core-matched technology (CMT) was evaluated in vitro and in vivo in mice. The core-matched NEs showed entrapment efficiency of >90% and were of nanoscale particle size and negative zeta-potential. The combined core-matched NEs exhibited concentration and time-dependent cytotoxicity against PTX-sensitive KB-3-1 cells and PTX-resistant KB-8-5 cells as well as an obviously increased G₂/M phase block. The improvements in therapeutic response over either PTX-VE or 5-FU-TPGS therapy alone were demonstrated by the ability to effectively induce the apoptosis of tumor cells via up-regulation of tumor suppressor p53 and β -tubulin and by the significant inhibition of cell cycle progression. The combination therapy led to dramatic inhibition of tumor growth with little toxicity in vivo, especially in the PTX-resistant KB-8-5 tumors, whereas Taxol had little therapeutic effect. This was mainly ascribed to the synergism of PTX and 5-FU and the reverse of MDR by the inhibition of ATPase activity by VE and TPGS. Coencapsulation of two chemotherapeutic agents with different mechanisms allows simultaneous interruption of diverse anticancer pathways, resulting in increased therapeutic response and low toxicity. The CMT markedly facilitated the long circulation of PTX and 5-FU, which was closely associated with the high accumulation of chemotherapeutic agents within the tumors and the improvement of antitumor efficacy. The current study demonstrated the feasibility of incorporating PTX and 5-FU targeting to different pathways into a single core-matched NE for the reversal of MDR and synergism in cancer therapy.

KEYWORDS: codelivery, paclitaxel, 5-fluorouracil, core-matched nanoemulsions, multidrug resistance



1. INTRODUCTION

There is growing evidence that drug combinations can be more effective than the sum of individual drug effects.¹ One course of therapy that demonstrated this theory is the administration of paclitaxel (PTX) combined with 5-fluorouracil (5-FU) to patients with gastric, breast, pancreatic, and other types of cancer,^{2–6} each drug using a different mechanism to kill tumor cells. Although the use of combined drugs appears to be promising in cancer therapy, the problem of bioavailability is still encountered because the drugs are often removed from blood circulation by macrophages or other molecular components associated with drug clearance from circulation. In a conventional anticancer drug combination regimen, the combined drugs that have synergistic actions in vitro are injected into the blood together but will distribute and be eliminated independently of each other. For example, PTX and

5-FU have half-lives of 1 h and 7 min, respectively, in mice.^{7,8} The different pharmacokinetic properties make it impossible to control the molar ratio of the two drugs taken up by the same diseased cells. Drug carrier systems have been proposed to address this problem⁹ based on the knowledge that the pharmacokinetic characteristics of individual drugs will depend on the carriers.

Oil in water (O/W) nanoemulsions (NEs), a nanocarrier system, can offer various advantages to therapeutics and targeting, for example, improvements of the chemical and/or

Special Issue: Drug Delivery and Reversal of MDR

Received: December 26, 2013

Revised: March 28, 2014

Accepted: April 8, 2014

Published: April 8, 2014

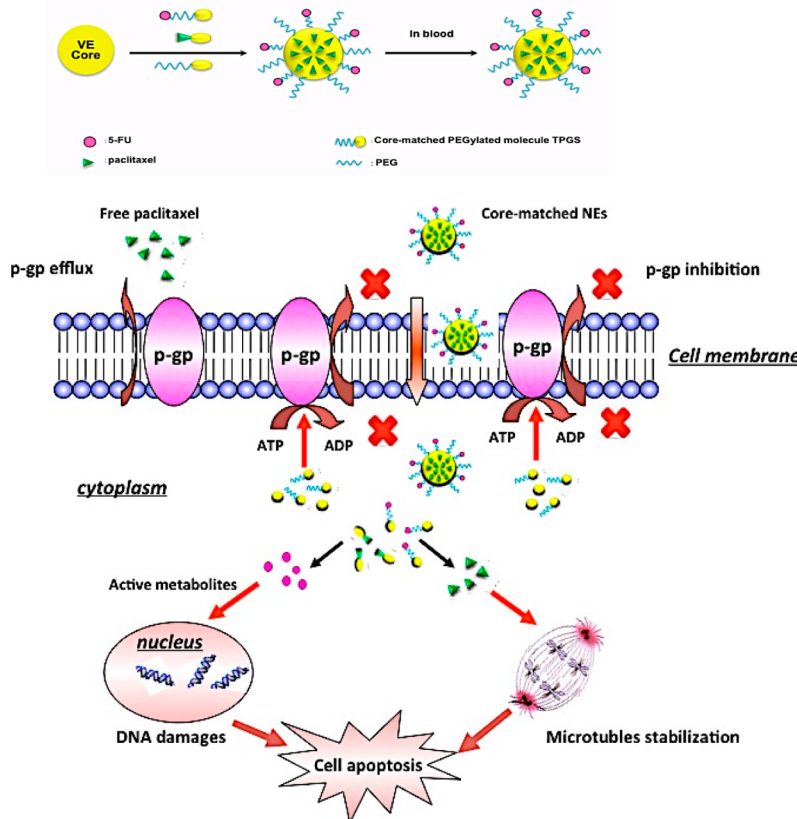


Figure 1. Schematic illustration of the core-matched nanoemulsions codelivering PTX and 5-FU to achieve the synergistic effects and reversal of MDR.

enzymatic stability of carried therapeutic agents, long-term colloidal stability, and ease of manufacture and scale-up.¹⁰ However, O/W NEs are designed to deliver hydrophobic drugs, which limit their application for the delivery of combined drugs, particularly for the combination of hydrophobic and hydrophilic anticancer drugs.

In order to improve the compatibility between the cargo and the core of NEs, in the present study, PTX and 5-FU were first conjugated with the functional vitamin E (VE) and tocopherol poly(ethylene glycol)succinate (TPGS), with VE and TPGS representing the oil core and PEGylated emulsifying agent in the NEs, respectively. The conjugated PTX and 5-FU were then loaded into the NEs based on the core-matched technology (CMT) proposed by our lab (Figure 1). The solubility and the stability of PTX and 5-FU in the core-matched NEs is increased due to more favorable interactions with the core by the functional molecules anchored to the NEs. PTX and 5-FU modified by VE and TPGS, respectively, can easily come into contact with the matched VE core contributing to the prevention of rapid drug release and the observation of satisfactory pharmacokinetic properties. The PEG stabilization also contributes to longer circulation times in vivo. In addition, PTX is known to be a substrate of P-glycoprotein (P-gp),¹¹ which has been involved in the multidrug resistance (MDR) of several cancers due to its overexpression. TPGS has been extensively investigated as an inhibitor of P-gp, and some TPGS-based nanoparticles or copolymers with similar structures have been proven to overcome MDR.^{12–14} Our previous study has also reported that VE causes significant reversal of MDR due to the inhibition of ATPase activity.¹⁵ Consequently, the conjugated PTX-VE and 5-FU-TPGS can

not only be encapsulated into a single nanocarrier to produce synergism by CMT but also reverse MDR in cancer treatment (Figure 1).

Our aim was to design core-matched NEs with the following functions: (1) ability to codeliver hydrophilic and hydrophobic anticancer drugs effectively; (2) improvement of the poor pharmacokinetics of PTX and 5-FU by promoting long circulation times and synergistic effects in vivo; (3) reversal of resistance to PTX by enhancing its antitumor activity.

2. EXPERIMENTAL SECTION

2.1. Materials. PTX was purchased from Lc Laboratories (Woburn, MA). PTX-VE and 5-FU-TPGS were synthesized in our lab (Figure 2). The synthesis and characterization of PTX-VE and 5-FU-TPGS is provided in the Supporting Information (Figures S1–S4). Paclitaxel injection (Taxol) was manufactured by Ben Venue Laboratories, Inc. (Bedford, OH). 5-Fluorouracil injection was purchased from APP Pharmaceuticals, LLC (Schaumburg, IL). Antibodies against p-S3, β-tubulin, P-gp, GAPDH, and horseradish peroxidase (HRP)-conjugated anti-mouse or anti-rabbit whole IgG were obtained from Santa Cruz Biotechnology (San Diego, CA). DeadEnd Fluorometric TUNEL assay kits were obtained from Promega (Madison, WI). Other chemicals were purchased from Sigma-Aldrich (St. Louis, MO).

KB-3-1 and KB-8-5 cells originally obtained from American Type Culture Collection (ATCC) (Manassas, VA) were maintained in RPMI 1640 and DMEM medium (Invitrogen, Carlsbad, CA) containing 10% fetal bovine serum (Invitrogen, Carlsbad, CA), 100 unit/mL penicillin, and 100 µg/mL

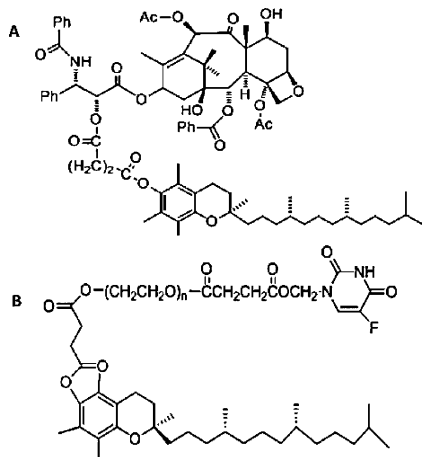


Figure 2. Chemical structures and synthetic design of PTX-VE (A) and 5-FU-TPGS (B).

streptomycin (Invitrogen, Carlsbad, CA). Cells were cultivated in a humidified incubator at 37 °C and 5% CO₂.

Mice were purchased from the National Cancer Institute (Bethesda, MD). All experiments performed on animals were in accordance with and approved by the Institutional Animal Care and Use Committee at the University of North Carolina at Chapel Hill.

2.2. Preparation of Core-Matched NE. PTX-VE, 5-FU-TPGS, TPGS, and VE were first dissolved in chloroform. Fifty microliters of PTX-VE (10 mg/mL), TPGS (50 mg/mL), and VE (150 mg/mL) and 125 μL of 5-FU-TPGS (15 mg/mL) were then separately withdrawn on ice and added to an Eppendorf tube with a screw cap. The chloroform was evaporated under nitrogen gas, and trace amounts of chloroform were further removed by keeping the mixture under vacuum in a desiccator for 1 h. Following the addition of 1 mL of distilled water, the mixture was sonicated using a sonic dismembrator model 100 (Fisher Scientific, Pittsburgh, PA) to produce the NE. In order to obtain a more homogeneous and fine particle size NE, the mixture was homogenized in a Bullet Blender (Next Advance, Averill Park, NY) using zirconium oxide beads (1:2; 1.0 mm diameter/0.5 mm diameter). The instrument was set at the eighth speed for 15 min. Particle size and zeta-potential of the NEs were determined by dynamic light scattering measurements using a Malvern ZetaSizer Nano series instrument (Westborough, MA). The loading efficiency of PTX-VE was assessed, following high-speed centrifugation to separate the free drug from NEs, using a liquid scintillation analyzer (TRI-CARB, Packard Bioscience Company, Waltham, MA). The shape and surface morphology of the NEs were observed using a JEOL 100CX transmission electron microscope (Tokyo, Japan). Prepared samples (5 μL) were dropped onto a 200 mesh carbon-coated copper grid (Ted Pella, Inc., Redding, CA) and then wicked off from the grid after 3 min. Grids were then stained with 1% uranyl acetate (5 μL) for 10–15 s and wicked for TEM. All TEM images were acquired at an accelerating voltage of 100 kV.

2.3. Cytotoxicity Assay. KB-3-1 and KB-8-5 cells were seeded into 96-well plates at a density of 1 × 10⁴ cells per well and allowed to adhere overnight. Various concentrations of drug or formulation were added to the plates for 48 h. Following incubation, 20 μL of MTT reagent (5 mg/mL in PBS) was added to the culture medium and the cells were incubated for an additional 4 h at 37 °C. The culture medium

was then carefully removed, and 200 μL of DMSO was added to the wells to dissolve the formazan. UV absorbance was measured at 570 nm using a Bio-Rad microplate imaging system (Hercules, CA), and results were expressed as % cell viability (OD of treated group/OD of control group × 100).

2.4. Cell Cycle Arrest. KB-8-5 cells growing exponentially were seeded at 1 × 10⁵ cells/mL in 12-well plates. Cells were treated with PTX-VE NE, 5-FU-TPGS NE, or combined NE for 48 h. The PBS solution served as the control. Ice-cold 70% ethanol was used to fix the cells at 4 °C overnight. After centrifugation and removal of the supernatant, the cells were resuspended with 1 mL of staining buffer and washed once. After repeat resuspension, the cells were incubated with 10 μL of RNase A (10 mg/mL) at 37 °C for 30 min and then stained with 5 μL of propidium iodide (1 mg/mL) at room temperature for 30 min. The cell cycle analysis was performed using a FACSCanto flow cytometry system (BD Biosciences, San Jose, CA).

2.5. Western Blot Analysis. Adherent cells in culture dishes were washed with ice-cold PBS, scraped using a cold plastic cell scraper, and then gently transferred, in suspension, to a precooled microcentrifuge tube. Whole cell lysates were extracted with RIPA buffer, and the protein concentration was measured using a Pierce BCA protein assay kit (Thermo Scientific, Rockford, IL). For each sample, approximately 50 μg of protein was separated on a NuPAGE 12% SDS-polyacrylamide gel and then transferred to a polyvinylidene difluoride (PVDF) membrane (Bio-Rad, Hercules, CA). The membrane was blocked with 5% skimmed milk in PBS for 1 h. After incubation with primary antibody at 4 °C overnight, it was washed with PBST (0.2% Tween 80 in PBS) and then incubated with secondary antibody for 1 h. Antibodies against P-gp, p-S3, β-tubulin, and GAPDH were used at 1:2000, 1:200, 1:500, and 1:2000 dilutions, respectively. An anti-mouse antibody conjugated with HRP at a dilution of 1:10000 or an anti-rabbit IgG at a dilution of 1:2000 served as the secondary antibodies in the experiment. The specific protein bands were visualized using a chemiluminescence kit (Thermo Scientific, Rockford, IL). Chemiluminescent signals were detected using high-performance chemiluminescence film (GE Healthcare Biosciences, Pittsburgh, PA).

2.6. Antitumor Activity in Vivo. In vivo antitumor activity was evaluated in KB-3-1 and KB-8-5 bearing nude mice. Female nude mice (6–8 weeks) were used in all studies. Nude mice were inoculated with 5 × 10⁶ KB-3-1 cells or KB-8-5 cells injected subcutaneously into their right or left flanks to establish the xenograft model. Once the tumor mass in the xenograft was established, mice were randomly divided into 5 groups (5 mice per group) and were injected, in the tail vein, with normal saline (the control group), Taxol, PTX-VE NE, 5-FU-TPGS NE, or PTX-VE combined 5-FU-TPGS NE. Drug doses of 5 mg/kg PTX, 8 mg/kg PTX-VE, and 30 mg/kg 5-FU-TPGS were used for all treatments. Therapy was continued at days 3, 5, 7, and 9 (five doses in total). Tumor volumes were calculated as (length × width²)/2 from measurements taken every second day. Mice were sacrificed when the length of the tumor reached 2 cm. Toxicity of the formulations was determined by monitoring mice behavior and weight loss and by HE staining.

2.7. TUNEL Assay. KB-3-1 and KB-8-5 tumor-bearing nude mice were given IV injections of the five formulations on days 1, 3, 5, 7, and 9. Mice were sacrificed 24 h after the final injection. Tumors were fixed in 10% formalin for at least 24 h

before being embedded in paraffin and sectioned at a thickness of 5 μm . In vivo tumor cell apoptosis was determined using the TUNEL assay. The TUNEL staining was performed as recommended by the manufacturer (Promega, Madison, WI), and DAPI mounting medium was dropped on the sections for nucleus staining. Images of TUNEL-stained tumor sections were taken with a fluorescence microscope (Nikon Corp., Tokyo, Japan). The TUNEL-positive cells were counted using ImageJ software (National Institutes of Health, Bethesda, MD).

2.8. Pharmacokinetics. Female CD-1 mice (18–22 g) were intravenously injected with PTX-VE and 5-FU-TPGS combined NE, Taxol, or 5-FU injection at a volume of 0.2 mL (8 mg/kg PTX-VE, 5 mg/kg PTX, and 2.22 mg/kg 5-FU). Each mouse received 1 μCi tritium-labeled PTX-VE or PTX, 5-FU, or 5-FU-TPGS. A 10–20 mg blood sample was collected at the predetermined time. Blood samples were digested in tissue solubilizer (GE Healthcare Bio-Sciences, Pittsburgh, PA) at a ratio of 1 mg/10 μL . Then, 200 μL of hydrogen peroxide (30%) was added to 100 μL of sample for decolorization. Following this, a scintillation cocktail (Ultima Gold XR, PerkinElmer, Waltham, MA) was added and the decolorized samples were stored in the dark for 40 min. The radioactivity was then quantified using a liquid scintillation analyzer (TRI-CARB, Packard Bioscience Company, Waltham, MA). The concentrations of drugs in the samples were determined, following subtraction of blank background radioactivity, by extrapolation from standard calibration curves. Pharmacokinetic parameters were calculated by DAS 2.1.1 software.

2.9. Statistical Analysis. Data were expressed as mean \pm SD. The statistical significance of group differences was analyzed using the Student's *t*-test, and a value of $p < 0.05$ was considered significant.

3. RESULTS AND DISCUSSION

3.1. Characterization of the NEs Codelivering Hydrophobic and Hydrophilic Anticancer Agents. In the study, the average particle size of the core-matched NEs was 82 nm with a PDI of 0.165, which was considered effective for passive targeting of tumors. The morphology of the core-matched NEs examined by TEM (Figure 3 and Figure S5) exhibited a uniform and spherical shape. The loading efficiency of PTX-VE in the core-matched NEs was >95%, 6-fold more than that of PTX alone, due to the solubility of PTX-VE in the VE oil phase. The combined core-matched NEs had a negative zeta-potential of 11.6 mV. The in vitro release of PTX-VE in the core-matched NEs was slow (Figure S6), and no burst effect

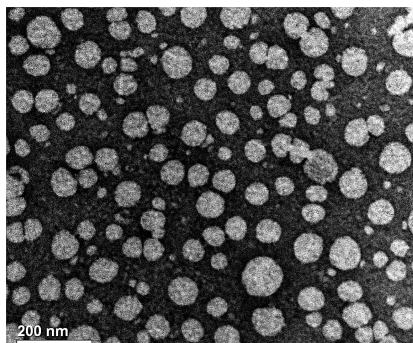


Figure 3. TEM images of the combined PTX-VE and 5-FU-TPGS core-matched NEs.

occurred. Therefore, the core-matched NEs effectively avoid problems reported with other PTX formulations, including low entrapment efficiency, drug instability, and rapid drug leakage.¹⁶

Many therapeutic agents hitherto have not been successful due to their limited ability to reach the target tissue. Thus, a drug delivery strategy that selectively targets the malignant tumor is necessary.¹⁷ The core-matched NEs have properties suited to synchronously delivering, in vitro and in vivo, both hydrophobic and hydrophilic anticancer drugs because of their nanoscale size and their stability within the matched core.

3.2. Dual Delivery of PTX and 5-FU To Achieve Synergism and Overcome PTX Resistance in MDR Cancer Cell Line. Data in Figure 4A,B show that PTX-VE and 5-FU-TPGS had a toxic effect in both PTX-sensitive and

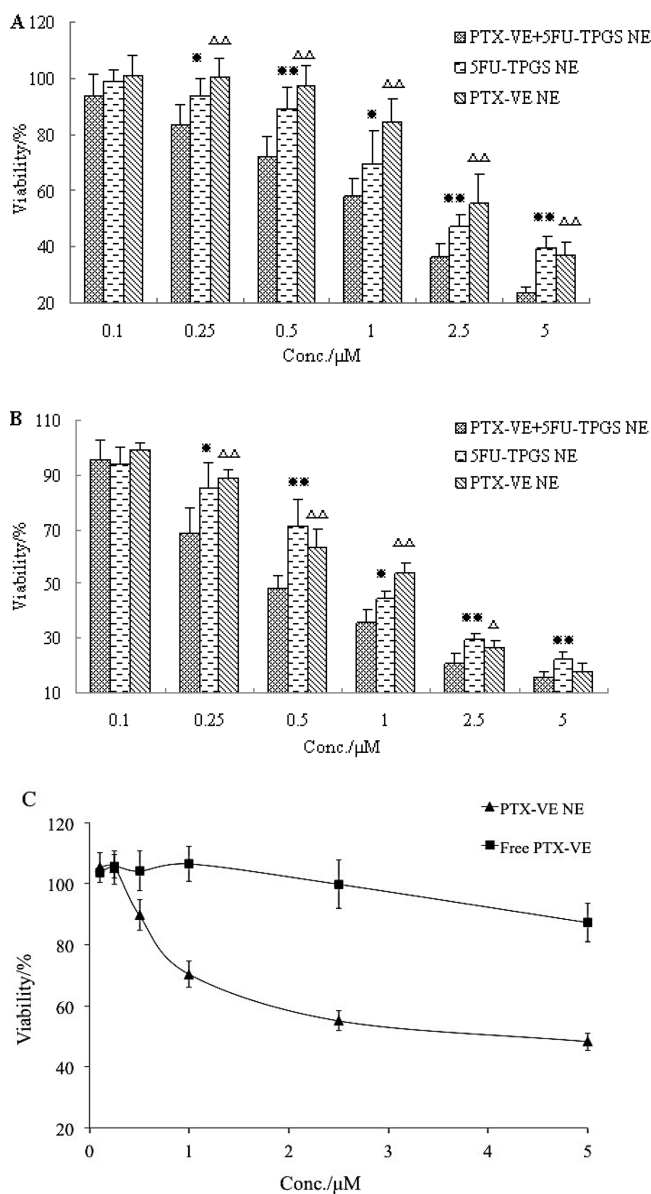


Figure 4. Cytotoxicity of PTX-VE NE, 5-FU-TPGS NE, and the combined NE against (A) KB-3-1 cells, (B) KB-8-5 cells, and (C) free PTX-VE and PTX-VE NE in KB-8-5 cells (mean \pm SD, $n = 6$). The concentrations on the x -axis represent the concentrations of PTX-VE. The concentrations of 5-FU-TPGS used were 2.9-fold lower than those of the PTX-VE.

-resistant cells. In particular, the combined core-matched NEs had the most significant cytotoxicity in both cell lines compared with the NE of the individual prodrug. The IC_{50} of PTX-VE NE in the resistant KB-8-5 cells was $1.27 \mu\text{M}$, lower than that in the sensitive KB-3-1 cells ($2.67 \mu\text{M}$). However, the IC_{50} of PTX in resistant cells was as much as 3 times that determined in sensitive cells (see Table 1). It was shown that the codelivery of

Table 1. IC_{50} for KB-8-5 and KB-3-1 Cells Treated with the Individual or Combined Drug NEs

$IC_{50} (\mu\text{M})$	KB-8-5	KB-3-1	resistance index
PTX-VE NEs	1.27	2.67	0.48
5-FU-TPGS NEs	1.19	2.60	0.46
PTX-VE + 5-FU-TPGS NEs	0.54	1.38	0.39
PTX	0.080	0.027	2.96

PTX-VE and 5-FU-TPGS in one single drug carrier could improve the sensitivity of PTX in resistant cells through the reversal of MDR via VE and TPGS inhibiting the ATPase activity. The *in vitro* cytotoxicity assay revealed that the combined core-matched NEs improved the ability of the individual prodrugs to cause decreased viability of both sensitive and resistant KB cells. The cytotoxicity of free PTX-VE was not greater than that of PTX-VE core-matched NEs (see Figure 4C) due to its inability to transport through the cell membrane following its precipitation from DMSO after addition to the 96-well plate. The result also showed that the core-matched NE carrier plays a vital role in the delivery of water-insoluble PTX-VE *in vivo* and *in vitro*.

The synergism of PTX-VE and 5-FU-TPGS in cytotoxicity was assessed by the Chou-Talalay method.¹⁸ The combination index was calculated by the following equation: CI (combination index) = $(D_1/(D_x)_1 + (D_2/(D_x)_2)$, where D_x is the dose of one compound alone required to produce an effect (IC_{50}) and $(D)_1$ and $(D)_2$ are the doses of compounds 1 and 2 necessary to produce the same effect in combination. The CI values calculated for KB-8-5 and KB-3-1 cells, respectively, were 0.9 and 1.0. The CI theorem of Chou-Talalay offers quantitative definition for additive effect (CI = 1), synergism (CI < 1), and antagonism (CI > 1) in drug combinations.¹⁸ The results indicated that the combined NEs have a synergistic effect on resistant KB-8-5 cells and an additive effect on sensitive KB-3-1 cells. This could be ascribed to the reversal of MDR produced by TPGS and VE.

Cell cycle checkpoints are used to monitor and regulate the progress of the cell cycle. Two main checkpoints exist: the G₁/S

checkpoint and the G₂/M checkpoint.¹⁹ It is known that PTX can arrest sensitive tumor cells at the G₂/M phase by an unusual stabilization of the microtubule.²⁰ When resistant KB-8-5 cells were treated with PTX-VE NE, cells of the G₂/M phase increased from 27.3% in the untreated group to 52.6% (Figure 5). The result means that PTX-VE was converted to the parent drug PTX, which blocked the G₂/M phase in the cell cycle, even within the resistant cells, resulting in the reversal of MDR.

It has been reported that 5-FU exhibits three modes of cell growth modulation, namely, loss or accumulation of S phase cells, G₂/M block, and G₁/S arrest.²¹ In our study, the G₂/M phase arrest was evident in KB-8-5 cells treated with 5-FU-TPGS; 53.2% of cells were arrested probably because cells proficient in DNA mismatch repair showed marked modulation in the G₂/M phase.²¹ Furthermore, the combined CME showed the most significant effect on the cell cycle, with 61.4% of cells being arrested at the G₂/M phase.

Tubulin is the target for anticancer drugs such as Taxol, Tepotaxane, vinblastine, and vincristine.²² Paclitaxel has the ability to bind to β -tubulin and unusually stabilize the microtubules. Previous studies have shown that PTX can enhance the expression of β -tubulin in sensitive KB-3-1 cell lines but not in PTX-resistant cell lines.²³ In the present study, we found that PTX-VE CME and the combined core-matched NEs upregulated the level of β -tubulin in the resistant KB-8-5 cell line (Figure 6). The result is consistent with the cell cycle assay

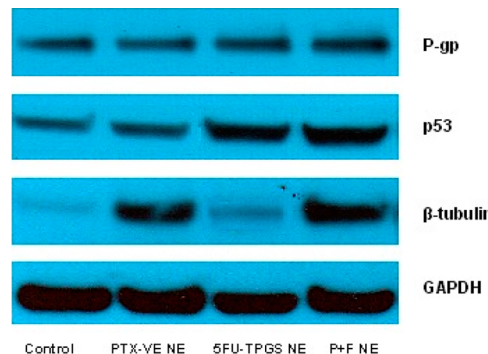


Figure 6. Western blotting assays for P-gp, β -tubulin, and p53 protein extracted from KB-8-5 cells treated with PTX-VE NEs, 5-FU-TPGS NEs, or the combined NEs for 48 h.

above, which showed G₂/M phase enhancement. P-gp, a marker for MDR, showed no change in both the untreated and

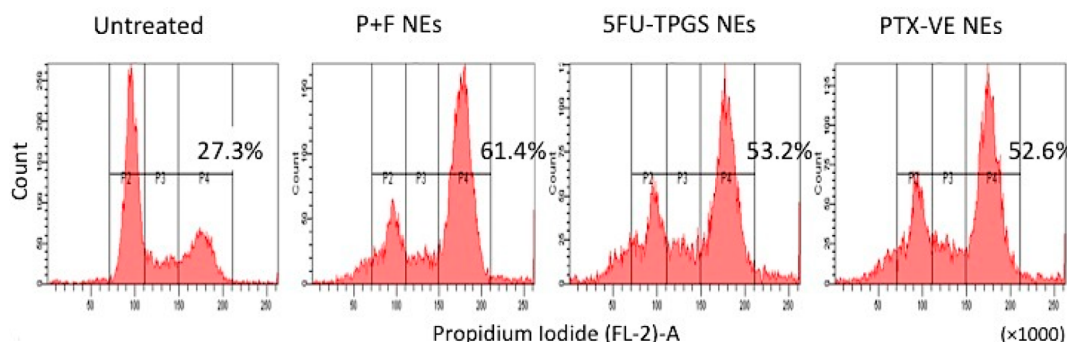


Figure 5. Cell cycle assays. Typical flow cytometric diagrams and G₂/M phase distribution of the KB-8-5 cells treated with PTX-VE NEs, 5-FU-TPGS NEs, and the combined NEs for 48 h (mean \pm SD, $n = 3$).

treated groups. Previous studies have elucidated that VE and TPGS reverse MDR by inhibiting the ATPase activity of P-gp rather than by regulating P-gp expression.¹⁵

The p53 tumor suppressor is a principal mediator of growth arrest, senescence, and apoptosis in response to a broad range of cellular damage. The p53 can initiate apoptosis if DNA damage proves to be irreparable.^{24,25} 5-FU exerts its anticancer effects through incorporation of its metabolites into RNA and DNA interfering with their normal functions. Our previous studies have shown that both 5-FU and 5-FU–PGS can increase the expression of p53.²³ Figure 6 shows that 5-FU–PGS core-matched NEs and the combined core-matched NEs facilitate the up-regulation of p53. This up-regulation is consistent with the reported ability of p53 to induce cell cycle arrest at the G₂/M boundary of the cell cycle.²⁶

3.3. Combinational Dlivery of PTX and 5-FU Leading to Synergistic Inhibition in Mouse Xenograft Model. As shown in Figure 7A, the reductions in tumor volume observed in nude mice treated with PTX–VE or 5-FU–TPGS core-matched NEs compared to control were not significant. A synergistic effect was observed in the combined core-matched NEs, which exhibited significant inhibition of tumor growth

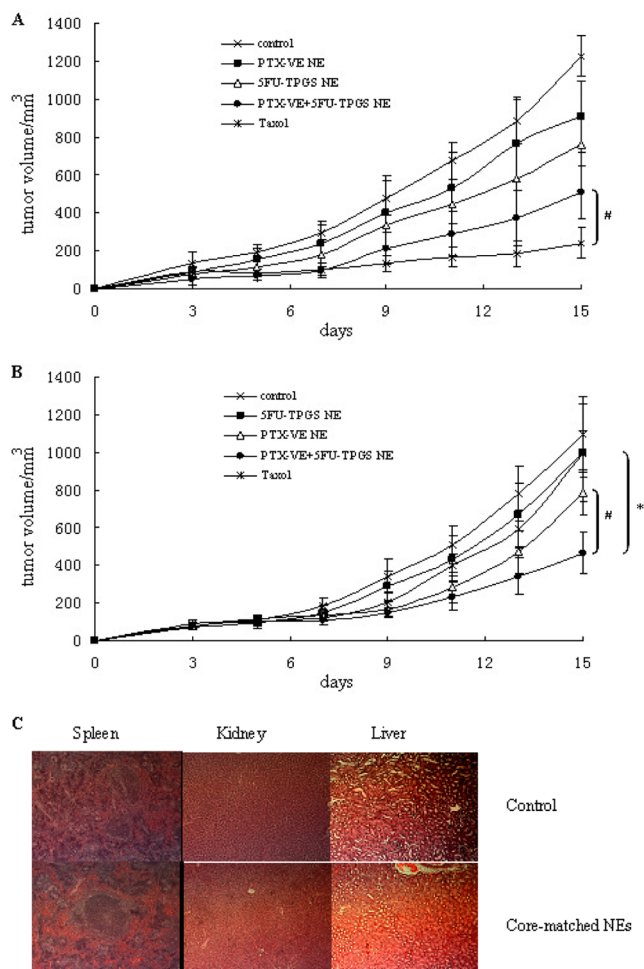


Figure 7. Tumor growth inhibition in subcutaneous tumor models of (A) KB-3-1 cells and (B) KB-8-5 cells. Tissue HE staining (C) after injection of the combined NEs, via the tail vein, every second day for 10 days. All data are expressed as mean \pm SD ($n = 5$); * $p < 0.05$ for combined NEs vs the individual NEs and # $p < 0.05$ for combined NEs vs the group treated with Taxol.

compared to the control group. However, Taxol showed a significantly reduced KB-3-1 tumor volume when compared to the other four groups. There were two supposed reasons for this. One was that KB-3-1 is a PTX-sensitive cell line, and the other is that the slow hydrolysis rate of PTX–VE resulted in slower inhibition of tumor growth.

Advantageous properties of the core-matched NEs loaded with both prodrugs were observed in the nude mice bearing resistant KB-8-5 tumors (Figure 7B). The results showed that the core-matched NEs were able to significantly inhibit the KB-8-5 tumor growth compared with the other four groups (tumor growth was reduced by 57.7% [t -test, $p < 0.05$]). It was thought that there were several reasons for this improved therapeutic effect. First, the core-matched technology prolonged the circulation of drug *in vivo* (data provided in pharmacokinetics study), facilitating greater drug accumulation in the tumor. Second, the codelivery of PTX and 5-FU in the prodrug form based on core-matched technology produced a synergistic effect. Third, VE and TPGS included in the prodrug and core-matched NE formulations help to reverse MDR.

Side effects are one of the major problems of cancer chemotherapy. In this study, the toxicity of the combined core-matched NEs on liver, spleen, and kidney was investigated using HE staining after long-term treatment. Figure 7C showed no obvious damage observed in these tissues after treatment with the core-matched NEs. Consistently, there was no decrease in body weight or noticeable change in activity.

We focused on the mechanism through which PTX–VE and 5-FU–TPGS core-matched NEs caused the resistant tumor cell death. TUNEL is a common method for detecting apoptotic programmed cell death. As illustrated in Figure 8, PTX–VE and 5-FU–TPGS core-matched NEs induced the most effective apoptosis of cells in KB-8-5 xenograft tumors compared with

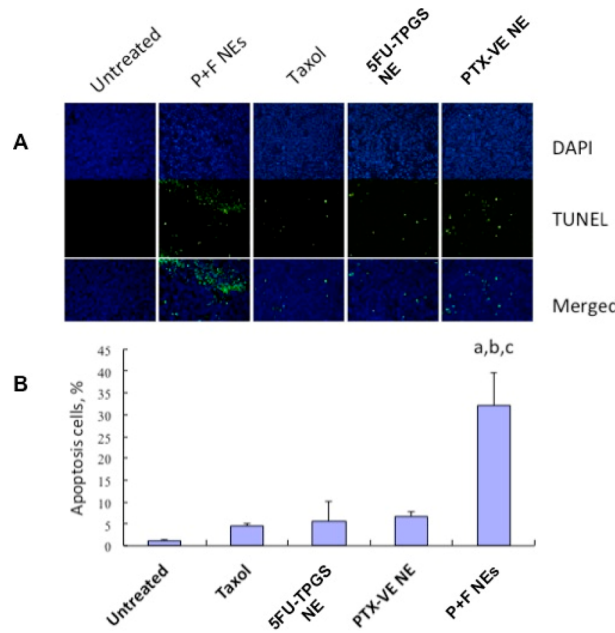


Figure 8. KB-8-5 tumor cell apoptosis induced by Taxol, PTX–VE NEs, 5-FU–TPGS NEs, and the combined NEs. (A) TUNEL assay of the tumor sections from KB-8-5 tumor-bearing nude mice after a schedule of 5 doses. TUNEL-positive cells are shown as green dots, and the nuclei stained by DAPI are blue. (B) Qualification of apoptosis; ^a $p < 0.05$ vs the control, ^b $p < 0.05$ vs the group treated with Taxol, and ^c $p < 0.05$ vs the group treated with individual NEs.

the control and individual prodrug NEs. The percentage of apoptotic cells ($32.1 \pm 7.6\%$) for the combined NEs was 7-fold higher than for Taxol (Figure 8). The TUNEL assay for the sensitive KB-3-1 tumor cells indicated that Taxol was able to induce significant cell apoptosis compared with other groups (Figure S7). The results were consistent with the antitumor effect seen in the sensitive cell tumor (Figure 7A).

The p53 is involved in chemosensitivity, and the loss of p53 function has been reported to enhance cellular resistance to a number of chemotherapeutic agents.²⁷ The extraordinary enhancement of cell apoptosis, and hence reversal of MDR, observed in our study was ascribed to the up-regulation of p53 and the arrest of the G₂/M phase in the cell cycle.

3.4. Prolongation of the Circulation of Anticancer Drugs in the Core-Matched NEs in Vivo. Anticancer drugs gain access to solid tumors via the circulatory system and must penetrate through the extravascular space to reach cancer cells in sufficient concentration to cause lethal toxicity. PTX and 5-FU are both eliminated quickly after intravenous injection. These considerations will most likely result in limited distribution of chemotherapy drug in solid tumors and potentially give rise to clinical resistance. It is therefore necessary to improve delivery of the drug to the tumor and to prolong the blood circulation of the drug so that, aided by the EPR effect, lethal concentrations in the tumor cells can be achieved. It is known that PEG is the most widely used moiety for surface modification of nanoparticles, and PEGylation can effectively retard the rapid uptake of nanoparticles by the mononuclear phagocyte systems.^{28,29} For this reason, 5-FU in our study was conjugated with TPGS and TPGS was also included in the core-matched NEs.

As Figure 9A,B and Table 2 show, the AUC_(0→∞) of both PTX and 5-FU following the administration of the core-matched NEs was much higher than after administration of Taxol or 5-FU injection. The C_{max} of PTX in NEs was found to be 64.9 mg/L, whereas the C_{max} following administration of Taxol was 1.9 mg/L. The MRT_(0,t) of PTX from the core-matched NEs was 29.6 h, significantly higher than that following Taxol administration (1.3 h). This showed that PTX from core-matched NEs existed in vivo much longer than PTX from Taxol. Data in Table 2 show that the elimination of 5-FU after administration of core-matched NEs was also slower than after 5-FU injection. The half-life of 5-FU from the NEs was nearly 3.5 times longer than that of 5-FU following administration of the 5-FU injection. These results could be ascribed to the presence of PEGylated NE surfaces.

The results indicated that the core-matched NEs facilitate the long circulation of PTX and 5-FU, which is closely associated with the high accumulation of chemotherapeutic agents within tumors and the improvement of antitumor efficacy. Although the elimination of 5-FU in the core-matched NEs was more rapid than the elimination of PTX, it was still much improved when compared with the 5-FU injection (Figure 9B). The antitumor activity observed has also shown the benefit of the combinational delivery with respect to the pharmacokinetics. In order to prolong the circulation of 5-FU even more, in future studies, it is planned that the 5-FU be conjugated with VE in order to avoid its loss through shedding of PEG derivative from the interface of NEs.

4. CONCLUSIONS

Based on the core-matched technology proposed by our lab, PTX and 5-FU were coencapsulated into a single nanoemulsion

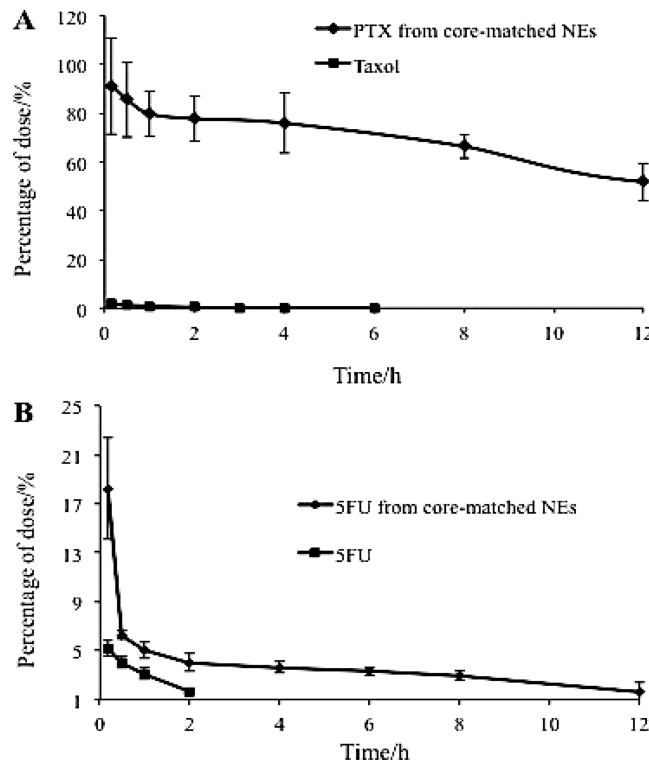


Figure 9. PK profiles of PTX (A) and 5-FU (B). The mice were injected intravenously with Taxol, 5-FU injection, or core-matched NEs (equal dose of 5 mg PTX/kg and 2.2 mg 5-FU/kg) containing 1 μ Ci of tritium-labeled PTX and 5-FU.

Table 2. Pharmacokinetic Parameters of PTX and 5-FU after Intravenous Injection ($n = 3$)

parameters	PTX-VE NPs	Taxol	5-FU-TPGS NPs	5-FU injection
AUC _(0-t) (mg·L ⁻¹ ·h)	2044	2.6	44.4	9.0
AUC _(0-∞) (mg·L ⁻¹ ·h)	2285	2.7	95.2	9.8
MRT _(0-t) (h)	29.6	1.3	4.4	1.3
MRT _(0-∞) (h)	2285	2.7	19.5	1.6
t _{1/2z} (h)	30.5	1.5	3.05	0.9
V _z (L/kg)	0.1	3.9	0.5	0.4
CL _z (L/h/kg)	0.002	1.8	0.02	0.2
C _{max} (mg/L)	64.9	1.9	18.2	5.2

in the form of prodrugs with high entrapment efficiency (>95%), good stability, and fine particle size (<90 nm). The combined core-matched NPs facilitate the long circulation of anticancer drugs in vivo, prevent drug loss through rapid clearance and metabolism, and render more drug accumulation in the tumor. Moreover, the codelivery of PTX and 5-FU in the single core-matched NPs contributes to reversal of MDR and the production of profound synergism. All of these advantages result in the significant inhibition of resistant tumor growth with no obvious toxicity.

ASSOCIATED CONTENT

S Supporting Information

Synthesis and characterization of PTX-VE and 5-FU-TPGS, release test from core-matched NPs in vitro, TEM images, particle size, and zeta-potential of the various NPs, TUNEL assay for sensitive cell tumor. This material is available free of charge via the Internet at <http://pubs.acs.org>.

AUTHOR INFORMATION

Corresponding Author

*E-mail: fliu@email.unc.edu. Phone: (919) 843-2277. Fax: (919) 966-0197.

Author Contributions

[†]Y.M. and D.L. contributed equally to this work.

Notes

The authors declare no competing financial interest.

ACKNOWLEDGMENTS

The study was funded by the National Cancer Institute, National Institutes of Health (SR01CA149387).

REFERENCES

- (1) Keith, C. T.; Boris, A. A.; Stockwell, B. R. Multicomponent therapeutics for networked systems. *Nat. Rev. Drug Discovery* **2005**, *4*, 71–78.
- (2) Cascinu, S.; Ficarelli, R.; Safi, M. A.; Graziano, F.; Catalano, G.; Cellerino, R. A phase I study of paclitaxel and 5-fluorouracil in advanced gastric cancer. *Eur. J. Cancer* **1997**, *33*, 1699–1702.
- (3) Kim, Y. H.; Shin, S. W.; Kim, B. S.; Kim, J. H.; Kim, J. G.; Mok, Y. J.; Kim, C. S.; Rhyu, H. S.; Hyun, J. H.; Kim, J. S. Paclitaxel, 5-fluorouracil, and cisplatin combination chemotherapy for the treatment of advanced gastric carcinoma. *Cancer* **1999**, *85*, 295–301.
- (4) Paul, D. M.; Garrett, A. M.; Meshad, M.; DeVore, R. D.; Porter, L. L.; Johnson, D. H. Paclitaxel and 5-fluorouracil in metastatic breast cancer: the US experience. *Semin. Oncol.* **1996**, *23*, 48–52.
- (5) Smorenburg, C. H.; Sparreboom, A.; Bontenbal, M.; Verweij, J. Combination chemotherapy of the taxanes and antimetabolites: its use and limitations. *Eur. J. Cancer* **2001**, *37*, 2310–2323.
- (6) Kim, Y. J.; Bang, S.; Park, J. Y.; Park, S. W.; Chung, J. B.; Song, S. Y. Phase II study of 5-fluorouracil and paclitaxel in patients with gemcitabine-refractory pancreatic cancer. *Cancer Chemother. Pharmacol.* **2009**, *63*, 529–533.
- (7) Eiseman, J. L.; Eddington, N. D.; Leslie, J.; MacAuley, C.; Sentz, D. L.; Zuhowski, M.; Kujawa, J. M.; Young, D.; Egorin, M. J. Plasma pharmacokinetics and tissue distribution of paclitaxel in CD2F1 mice. *Cancer Chemother. Pharmacol.* **1994**, *34*, 465–471.
- (8) Li, Y.; Looney, G. A.; Kimler, B. F.; Hurwitz, A. Opiate effects on 5-fluorouracil disposition in mice. *Cancer Chemother. Pharmacol.* **1997**, *39*, 273–277.
- (9) Mayer, L. D.; Janoff, A. S. Optimizing combination chemotherapy by controlling drug ratios. *Mol. Interventions* **2007**, *7*, 216–223.
- (10) Date, A. A.; Desai, N.; Dixit, R.; Nagarsenker, M. Self-nanoemulsifying drug delivery systems: formulation insights, applications and advances. *Nanomedicine* **2010**, *5*, 1595–1616.
- (11) Dintaman, J. M.; Silverman, J. A. Inhibition of P-glycoprotein by D-alpha-tocopheryl polyethylene glycol 1000 succinate (TPGS). *Pharm. Res.* **1999**, *16*, 1550–1556.
- (12) Zhang, Z.; Tan, S.; Feng, S. S. Vitamin E TPGS as a molecular biomaterial for drug delivery. *Biomaterials* **2012**, *33*, 4889–4906.
- (13) Collnot, E. M.; Baldes, C.; Schaefer, U. F.; Edgar, K. J.; Wempe, M. F.; Lehr, C. M. Vitamin E TPGS P-glycoprotein inhibition mechanism: influence on conformational flexibility, intracellular ATP levels, and role of time and site of access. *Mol. Pharmaceutics* **2010**, *7*, 642–651.
- (14) Collnot, E. M.; Baldes, C.; Wempe, M. F.; Kappl, R.; Huttermann, J.; Hyatt, J. A.; Edqar, K. J.; Schaefer, U. F.; Lehr, C. M. Mechanism of inhibition of P-glycoprotein mediated efflux by vitamin E TPGS: influence on ATPase activity and membrane fluidity. *Mol. Pharmaceutics* **2007**, *4*, 465–474.
- (15) Tang, J. L.; Fu, Q.; Wang, Y. J.; Racette, K.; Wang, D.; Liu, F. Vitamin E reverses multidrug resistance in vitro and in vivo. *Cancer Lett.* **2013**, *336*, 149–157.
- (16) Singla, A. K.; Garg, A.; Aggarwal, D. Paclitaxel and its formulations. *Int. J. Pharm.* **2002**, *235*, 179–192.
- (17) Sahoo, S. K.; Labhsetwar, V. Nanotech approaches to drug delivery and imaging. *Drug Discovery Today* **2003**, *8*, 1112–1120.
- (18) Chou, T. C. Drug combination studies and their synergy quantification using the Chou-Talalay method. *Cancer Res.* **2010**, *70*, 440–446.
- (19) Elledge, S. J. Cell cycle checkpoints: preventing an identity crisis. *Science* **1996**, *274*, 1664–1672.
- (20) Horwitz, S. B. Taxol (paclitaxel): mechanisms of action. *Ann. Oncol.* **1994**, *5*, S3–S6.
- (21) Tokunaga, E.; Oda, S.; Fukushima, M.; Maehara, Y.; Sugimachi, K. Differential growth inhibition by 5-fluorouracil in human colorectal carcinoma cell lines. *Eur. J. Cancer* **2000**, *36*, 1998–2006.
- (22) Jordan, A.; Hadfield, J. A.; Lawrence, N. J.; McGown, A. T. Tubulin as a target for anticancer drugs: agents which interact with the mitotic spindle. *Med. Res. Rev.* **1998**, *18*, 259–296.
- (23) Wang, D.; Tang, J. L.; Wang, Y. J.; Ramishetti, S.; Fu, Q.; Racette, K.; Liu, F. Multifunctional nanoparticles based on a single-molecule modification for the treatment of drug-resistant cancer. *Mol. Pharmacol.* **2013**, *10*, 1465–1469.
- (24) Pietsch, E. C.; Sykes, S. M.; McMahon, S. B.; Murphy, M. E. The p53 family and programmed cell death. *Oncogene* **2008**, *27*, 6507–6521.
- (25) Sheikh, M. S.; Fornace, A. J., Jr. Role of p53 family members in apoptosis. *J. Cell Physiol.* **2000**, *182*, 171–181.
- (26) Stewart, N.; Hicks, G. G.; Paraskevas, F.; Mowat, M. Evidence for a second cell cycle block at G2/M by p53. *Oncogene* **1995**, *10*, 109–115.
- (27) Lowe, S. W.; Ruley, H. E.; Jacks, T.; Housman, D. E. p53-Dependent apoptosis modulates the cytotoxicity of anticancer agents. *Cell* **1993**, *74*, 957–967.
- (28) Jokerst, J. V.; Lobovkina, T.; Zare, R. N.; Gambhir, S. S. Nanoparticle PEGylation for imaging and therapy. *Nanomedicine* **2011**, *6*, 715–728.
- (29) Li, S. D.; Huang, L. Nanoparticles evading the reticuloendothelial system: role of the supported bilayer. *Biochim. Biophys. Acta* **2009**, *1788*, 2259–2266.